

ORIGINAL RESEARCH



Identifying six chromatin remodeling-related genes as diagnostic biomarkers in sepsis using bioinformatic analyses

Yansong Miao^{1,†}, Ning Liu^{1,†}, Lifeng Xing¹, Bing Li¹, Wei Xiao¹, Junru Dai¹, Xuchang Qin¹, Yang He¹, Yiming Zhao¹, Zhonghua Chen¹, Li Hu¹, Lian Liu¹, Zhongheng Zhang^{1,*}

¹Department of Emergency Medicine, Sir Run-Run Shaw Hospital, Zhejiang University School of Medicine, 310016 Hangzhou, Zhejiang, China

***Correspondence**

zh_zhang1984@zju.edu.cn
(Zhongheng Zhang)

[†] These authors contributed equally.

Abstract

Background: Epigenetic modifications, such as chromatin remodeling, are critical in regulating sepsis immunity. Identifying differentially expressed chromatin remodeling-related genes (DE-CRRGs) may reveal potential therapeutic targets for sepsis. **Methods:** Using the GSE65682 dataset, we identified DE-CRRGs between sepsis and normal groups. Least absolute shrinkage and selection operator (LASSO) regression, support vector machine (SVM), and random forest algorithms were applied to screen hub genes. Immune cell infiltration was analyzed using cell type identification by estimating relative subsets of RNA transcripts (CIBERSORT), and ceRNA regulatory and co-expression networks were constructed. Potential drugs were predicted using the Drug Gene Interaction Database. **Results:** We identified 17 DE-CRRGs and six hub genes: spondin 2 (*SPON2*), transglutaminase 2 (*TGM2*), matrix metalloproteinase 9 (*MMP9*), DNA Methyltransferase 1 (*DNMT1*), lymphocyte antigen 96 (*LY96*), and forkhead box protein 1 (*FOXO1*). These genes were significantly correlated with immune cell infiltration, particularly activated natural killer (NK) cells, cluster of differentiation (CD)8 T cells, and plasma cells. The hub genes were involved in interleukin-18 signaling and cell development. Additionally, 62 potential drugs for sepsis treatment were predicted. **Conclusions:** These findings provide insights into the epigenetic regulation of sepsis and suggest potential therapeutic targets and drugs for intervention.

Keywords

Sepsis; Chromatin remodeling; Diagnostic markers; ceRNA regulatory network; Drug prediction

1. Introduction

Among intensive care unit patients, characterized by immune system imbalance due to pathogen invasion, ultimately resulting in severe organ dysfunction [1, 2]. The current diagnostic methods analyzing blood, urine, wound secretions, and mucus—frequently cause delays in diagnosis and intervention [3, 4]. Additionally, the mortality rate among critically ill sepsis patients remains high, and the key factors and mechanisms underlying their diagnosis are still not well understood.

Epigenetic modifications, including histone modifications, DNA methylation, and chromatin remodeling, are crucial for determining cell lineage during development. Alterations in these processes often promote embryonic tumorigenesis. Chromatin remodeling, the final step of epigenetic regulation, achieves a specific chromatin condensation state, facilitating the activity of chromatin remodeling agents at specific genomic sites [5, 6]. These modifications play an immunosuppressive role during the late stages of sepsis [7, 8].

Sirtuin 6 (*SIRT6*), which regulates chromatin remodeling, genome stability, and transcription, has been shown to influence mitochondrial dynamics and biogenesis and induce G₂/M cell cycle arrest, both related to the pathophysiology of sepsis [9]. Overexpression of the SWItch3-related gene, a chromatin remodeling factor, promotes M2 macrophage differentiation and suppresses interferon- γ production by natural killer (NK) cells, positively impacting sepsis prognosis [10]. These studies indicate that chromatin remodeling-related genes (CRRGs) play significant roles in sepsis and may serve as potential therapeutic targets for this disease.

This study used bioinformatics to identify prognostic biomarkers related to chromatin remodeling in sepsis and further elucidated their roles through functional and mechanistic analyses. These findings provide promising insights for enhancing the diagnosis and treatment of sepsis patients.

2. Materials and methods

2.1 Microarray data collection

The training set GSE65682 and the validation set GSE134347 were downloaded from the Gene Expression Omnibus (GEO) database (<https://www.ncbi.nlm.nih.gov/geo/>). GSE65682 contains data on 802 samples, with 42 normal and 760 patient samples. GSE134347 includes data on 83 normal and 155 patient samples. Additionally, 66 chromatin remodeling-related genes (CRRGs) were obtained from the GeneCards database (<http://www.genecards.org/>).

2.2 Functional analysis of target genes

Differentially expressed genes (DEGs) between the disease and normal groups in the GSE65682 dataset were evaluated using the “limma” package (screening criteria: $|\log_2(\text{fold change})| > 1$, $\text{adj.}p.\text{value} < 0.05$). Volcano and heat maps were generated using the “ggplot2” and “pheatmap” packages, respectively, to illustrate the differential gene expression [11]. Differentially expressed CRRGs (DE-CRRGs) were identified by intersecting the DEGs with the 66 CRRGs (score > 10). Gene Ontology (GO) and Kyoto Encyclopedia of Genes and Genomes (KEGG) enrichment analyses were conducted on DE-CRRGs using the “clusterProfiler” package [12].

2.3 Screening of biomarkers

Three different algorithms were used to identify biomarkers: least absolute shrinkage and selection operator (LASSO) regression analysis was performed using the “glmnet” package in R, with the family set to “binomial”; the support vector machine (SVM) classifier in the “e1071” package was used to narrow the gene range through 10-fold cross-validation; and random forest analysis was conducted using the “randomForest” package. Biomarkers were identified by intersecting the key genes obtained from these three algorithms. The expression of these biomarkers was verified using the training set, and receiver operating characteristic (ROC) curves were plotted to evaluate their performance.

2.4 Gene set enrichment analysis (GSEA) of biomarkers

Based on the median expression value, biomarkers were divided into high-expression and low-expression groups, and differential expression was analyzed using the R “limma” package. To identify the common functions and related pathways among many genes in DEGs, their $\log_2(\text{fold change})$ values were sorted from high to low, and gene set enrichment analysis (GSEA) was performed using the “clusterProfiler” package. Additionally, correlation analysis of biomarkers was conducted using the “corrplot” package [13].

2.5 Validation of diagnostic markers

To confirm the diagnostic efficacy of the identified biomarkers, the expression values of genes were extracted from the GSE134347 dataset to which ROC curve analysis was conducted, and the gene distribution results were visualized using a box plot.

2.6 Immune cell infiltration analysis

The infiltration of 22 types of immune cells in the sepsis and control groups was analyzed using “CIBERSORT” (<https://cibersort.stanford.edu/>) in R ($p < 0.05$). Differentially infiltrated immune cells were identified using a box plot. The correlation between the biomarkers and the 22 types of immune cells was analyzed and visualized using the “psych” package.

2.7 Construction of competing endogenous RNA (ceRNA) networks

MicroRNAs (miRNAs) upstream of the biomarker genes were predicted using the miRWalk database (<http://mirwalk.umm.uni-heidelberg.de/>). These predictions were then intersected with miRNAs interacting with the biomarkers, identified using miRDB, miRTarBase and TargetScan. Similarly, long non-coding RNAs (lncRNAs) were predicted using the Starbase database (<https://starbase.sysu.edu.cn/index.php>), and the ceRNA network was constructed. To analyze the interaction between biomarkers and other genes, a biomarker co-expression network was constructed using GeneMANIA (<http://genemania.org/>). Lastly, the functions of these biomarkers were predicted using Metascape.

2.8 Drug prediction

The biomarkers were input into the Drug Gene Interaction Database, and a network of model genes and molecules was constructed using Cytoscape to identify potential drugs or compounds for treating sepsis.

2.9 Statistical analysis

All statistical analyses were performed in R (<https://www.r-project.org/>, version 4.0.2). Data from the different groups were compared using the Wilcoxon rank-sum test, with $p < 0.05$ considered statistically significant.

3. Results

3.1 Analysis of DE-CRRGs in sepsis

Using the “limma” package, we analyzed the sepsis and normal groups in the GSE65682 dataset, based on which 1248 up-regulated and 2601 down-regulated genes were identified. These genes are shown *via* volcano plots and heatmaps (Fig. 1A,B). From these DEGs, we obtained 17 differentially expressed chromatin remodeling-related genes (DE-CRRGs) (Fig. 1C). Principal component analysis (PCA) showed a clear separation between the control and disease samples, with PC1 accounting for 18.34% of the variance and PC2 accounting for 15.36% (Fig. 1D).

3.2 Enrichment analysis of DE-CRRGs in sepsis

Enrichment analysis provided insights into the pathways and potential biological mechanisms of the enriched genes. The 17 DE-CRRGs were significantly enriched in 685 Gene Ontology

(GO) pathways, including response to lipopolysaccharide, platelet α -granule, and lipopolysaccharide binding, and 20 Kyoto Encyclopedia of Genes and Genomes (KEGG) pathways, such as cellular senescence, FOXO signaling, and the transforming growth factor- β (TGF β) signaling pathway (Fig. 1E,F).

3.3 Screening of hub genes

Three algorithms were used to further screen biomarkers. LASSO logistic regression selected strong correlation features and generated a cross-validation error diagram, identifying 11 characteristic genes: *SPON2*, ETS transcription factor

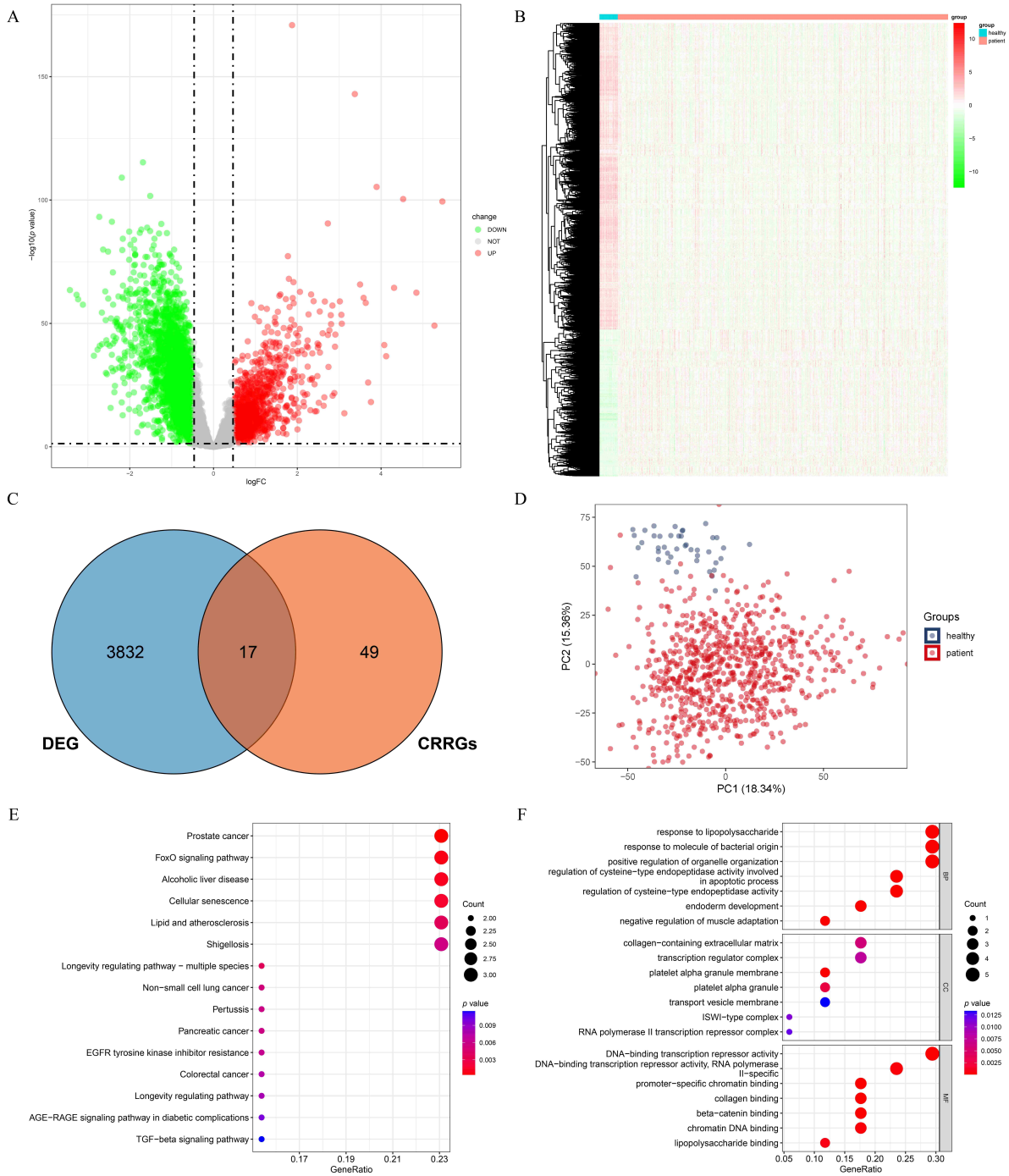


FIGURE 1. Screening and enrichment analysis of DE-CRRGs in sepsis. (A) Volcano plot of GSE65682. (B) Heatmap of GSE65682. (C) Venn diagram of DE-CRRGs. (D) Principal component analysis (PCA). (E) KEGG enrichment map of DE-CRRGs. (F) GO enrichment map of DE-CRRGs. Abbreviations: DE-CRRGs, differentially expressed chromatin remodeling-related genes; PCA, principal component analysis; KEGG, Kyoto Encyclopedia of Genes and Genomes; GO, Gene Ontology; $\log_2(\text{FC})$, log fold-changes; DEG, differentially expressed gene; CRRGs, chromatin remodeling-related genes; EGFR, epidermal growth factor receptor; AGE-RAGE, advanced glycation end products-receptor of advanced glycation end products; TGF, transforming growth factor; ISWI, imitation switch; BP, biological process; CC, cell composition; MF, molecular function.

ELK3 (*ELK3*), *TGM2*, *MMP9*, *DNMT1*, transforming growth factor alpha (*TGFA*), *LY96*, histone deacetylase 9 (*HDAC9*), *FOXO1* and alpha-synuclein (*SNCA*) (Fig. 2A). The SVM, a supervised machine learning technology, used recursion to sort features, identifying 13 genes with the best effect: *LY96*, *TGM2*, *SPON2*, *MMP9*, *SNCA*, *TGFA*, secreted protein acidic and rich in cysteine (*SPARC*), *DNMT1*, *FOXO1*, bromodomain PHD finger transcription factor (*BPTF*), *FOXO3*, adrenomedullin (*ADM*) and *ELK3* (Fig. 2B). Random forest analysis provided the error rate curve and the importance score of the characteristic genes, identifying nine genes with an importance score greater than 2: *DNMT1*, *SMAD3*, *MMP9*, *LY96*, *ADM*, *FOXO1*, *SPON2*, *TGM2* and *HDAC9* (Fig. 2C,D). The intersection of the results from these three algorithms yielded six hub genes: *SPON2*, *TGM2*, *MMP9*, *DNMT1*, *LY96* and *FOXO1* (Fig. 2E).

3.4 Verification of hub gene expression

The expression levels of the characteristic genes were verified in the training set, showing significant differences between the normal and sepsis groups (Fig. 3A). To validate the diagnostic ability of these hub genes, ROC curves were plotted, revealing an area under the curve (AUC) of approximately 0.8, thereby indicating that the six hub genes—*SPON2*, *TGM2*, *MMP9*, *DNMT1*, *LY96* and *FOXO1*—demonstrate high accuracy and specificity in diagnosing sepsis (Fig. 3B).

3.5 GSEA of hub genes

The biomarkers were divided into high- and low-expression groups based on the median expression value, and differential expression between these groups was analyzed. To facilitate GSEA, we sorted the $\log_2(\text{fold change})$ values from high to low, which allowed us to analyze the common functions and related pathways of many genes in DEGs. The abscissa represents genes, with each small vertical line indicating a gene. Overall, the pathways were either up-regulated or down-regulated. For each gene, we highlighted the top five up-regulated and downregulated pathways (Fig. 4A–F). Glycosaminoglycan biosynthesis-Heparan sulfate/Heparin, asthma, and allograft rejection were the biological pathways in which most biomarkers were co-enriched. The correlation map of the six hub genes was charted using the “corrplot” package in R. *FOXO1* showed the highest correlation with *TGM2*, while *SPON2* was significantly correlated with the other five genes (Fig. 4G).

3.6 Verification of hub gene expression and ROC curve

The ability of the six hub genes to distinguish between disease and normal samples was verified using box plots and ROC curves based on the GSE134347 dataset. The expression levels of the six hub genes differed significantly between the two groups (Fig. 5A). According to the ROC curves, the AUC values were as follows: *LY96* was 0.904 (95% confidence interval (CI): 0.863–0.941), *FOXO1* was 0.925 (95% CI: 0.890–0.956), *DNMT1* was 0.965 (95% CI: 0.938–0.988), *TGM2* was 0.804 (95% CI: 0.747–0.858), *SPON2*

was 0.677 (95% CI: 0.603–0.745), and *MMP9* was 0.965 (95% CI: 0.940–0.985). These results indicate that the six hub genes exhibit high accuracy and specificity in diagnosing sepsis (Fig. 5B).

3.7 Immune cell infiltration analysis

The development of sepsis is closely related to our immune response against pathogenic microorganisms. Therefore, we used CIBERSORT and LM22 gene sets to calculate the proportions of 22 types of immune cells in the normal and disease groups (Fig. 6A). The proportions of each immune cell in each sample, along with their statistical values, were obtained using CIBERSORT, excluding samples with $p > 0.05$. A violin plot of the 22 types of immune cells in the normal and disease groups was generated in R. The infiltration of 16 out of the 22 types of immune cells differed significantly between the two groups ($p < 0.01$). These differences indicate that the immune environments of normal and sepsis patients are distinct.

Additionally, we analyzed and visualized the correlation between the six hub genes and the proportions of the 22 types of immune cells (Fig. 6B). The hub genes showed significant correlations with activated NK cells, CD8 cells, and plasma cells.

3.8 ceRNA regulatory network of hub genes

The miRNA–lncRNA–mRNA regulatory network was constructed based on 4 miRNAs, 47 lncRNAs and mRNAs (Fig. 7A). Among the hub genes, *FOXO1* may be regulated by the lncRNA AL0503412 through its effects on hsa-miR-27a-3p and hsa-miR-27b-3p, forming a complex ceRNA network rather than involving a single RNA molecule.

The co-expression network of biomarkers was constructed using GeneMANIA (<http://genemania.org/>), and the interactions between the biomarkers and other genes were analyzed (Fig. 7B). Most of the 20 genes shared protein domains with the biomarkers. Notably, *GM2A* and *LY96*, as well as *CXCR4* and *SPON2*, showed a high correlation, although few gene pairs exhibited genetic interaction.

Furthermore, the function of these biomarkers was predicted using Metascape, and the results showed that they were primarily involved in interleukin-18 signaling, cellular response to biological stimuli, and positive regulation of cell development, among other pathways (Fig. 7C).

3.9 Drug prediction

The Drug Gene Interaction database was utilized to identify potential therapeutic drugs or compounds for sepsis based on the six hub genes. Using “Cytoscape”, we constructed a network of model genes and molecules. The predicted drug network comprised 62 drugs, with two drugs targeting two genes each (Fig. 8). In this network, the green nodes represent hub genes, and the pink nodes represent drug molecules. Curcumin was found to target both *MMP9* and *DNMT1*, while cisplatin could target *TGM2* and *DNMT1*. However, only eritoran tetrasodium was found to impact *LY96*.

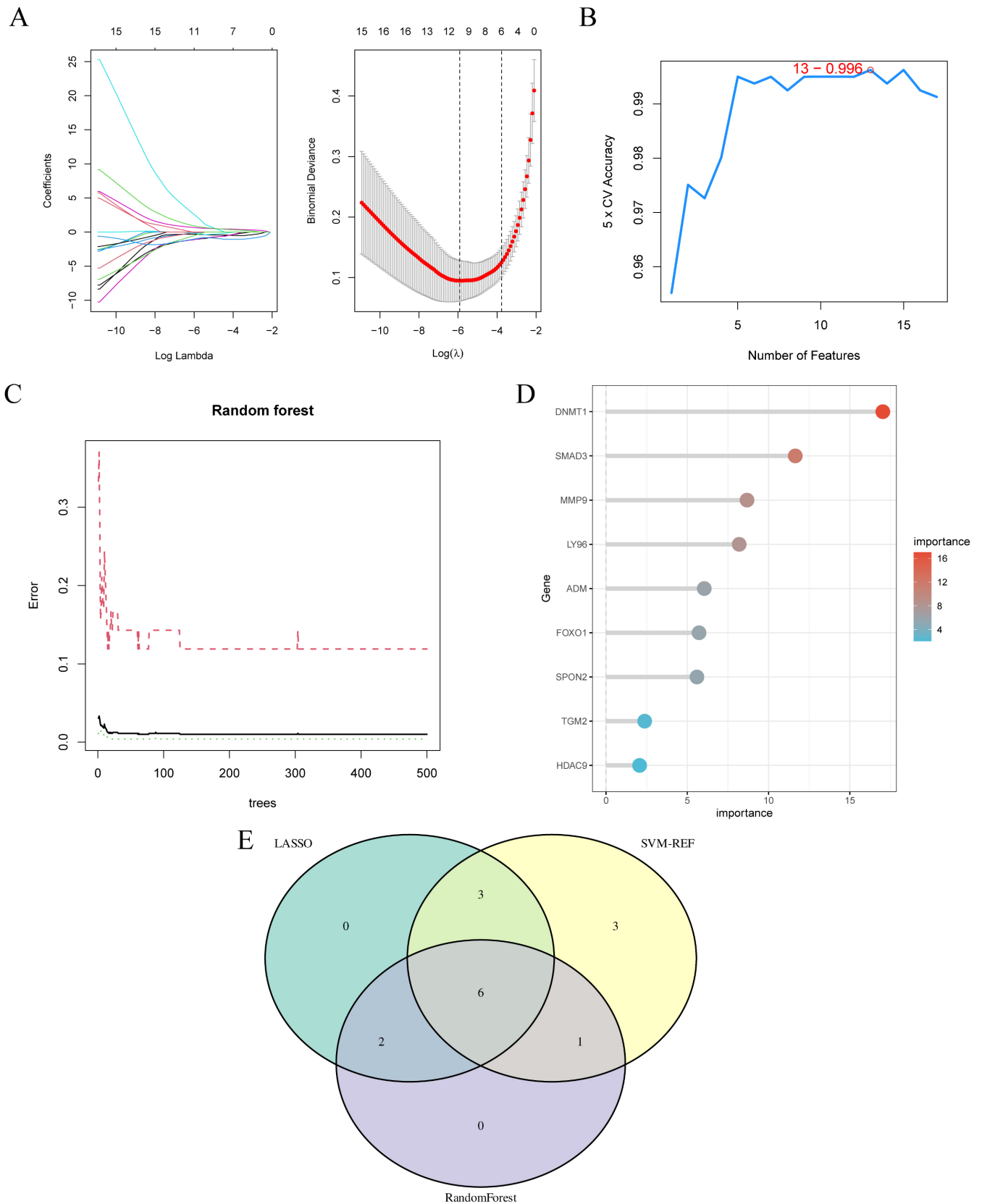


FIGURE 2. Screening of hub genes. (A) LASSO cross-validation error diagram. (B) Accuracy curve of the optimal characteristic genes. (C,D) Random forest screening of the characteristic genes. (E) Identification of hub genes using three machine-learning algorithms. LASSO, least absolute shrinkage and selection operator; CV, cross-validation; SVM-RFE, support vector machine-recursive feature elimination.

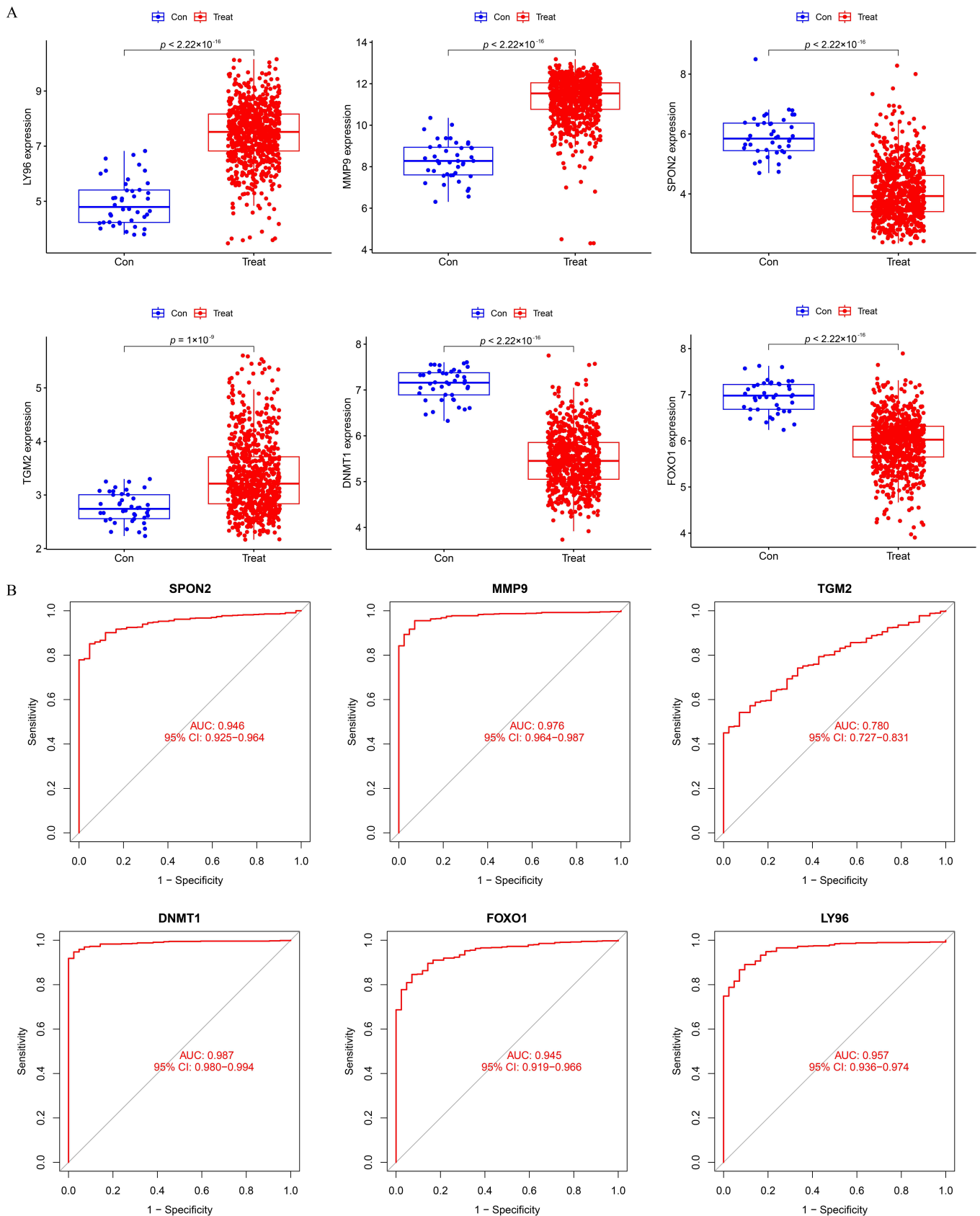


FIGURE 3. Hub gene expression in training set. (A) Expression analysis of the characteristic genes. (B) ROC curve in the training set. ROC, receiver operating characteristic. AUC, area under the curve; CI, confidence interval; *SPON2*, spindin 2; *MMP9*, matrix metalloproteinase 9; *TGM2*, transglutaminase 2; *DNMT1*, DNA methyltransferase 1; *FOXO1*, forkhead box protein 1; *LY96*, lymphocyte antigen 96.

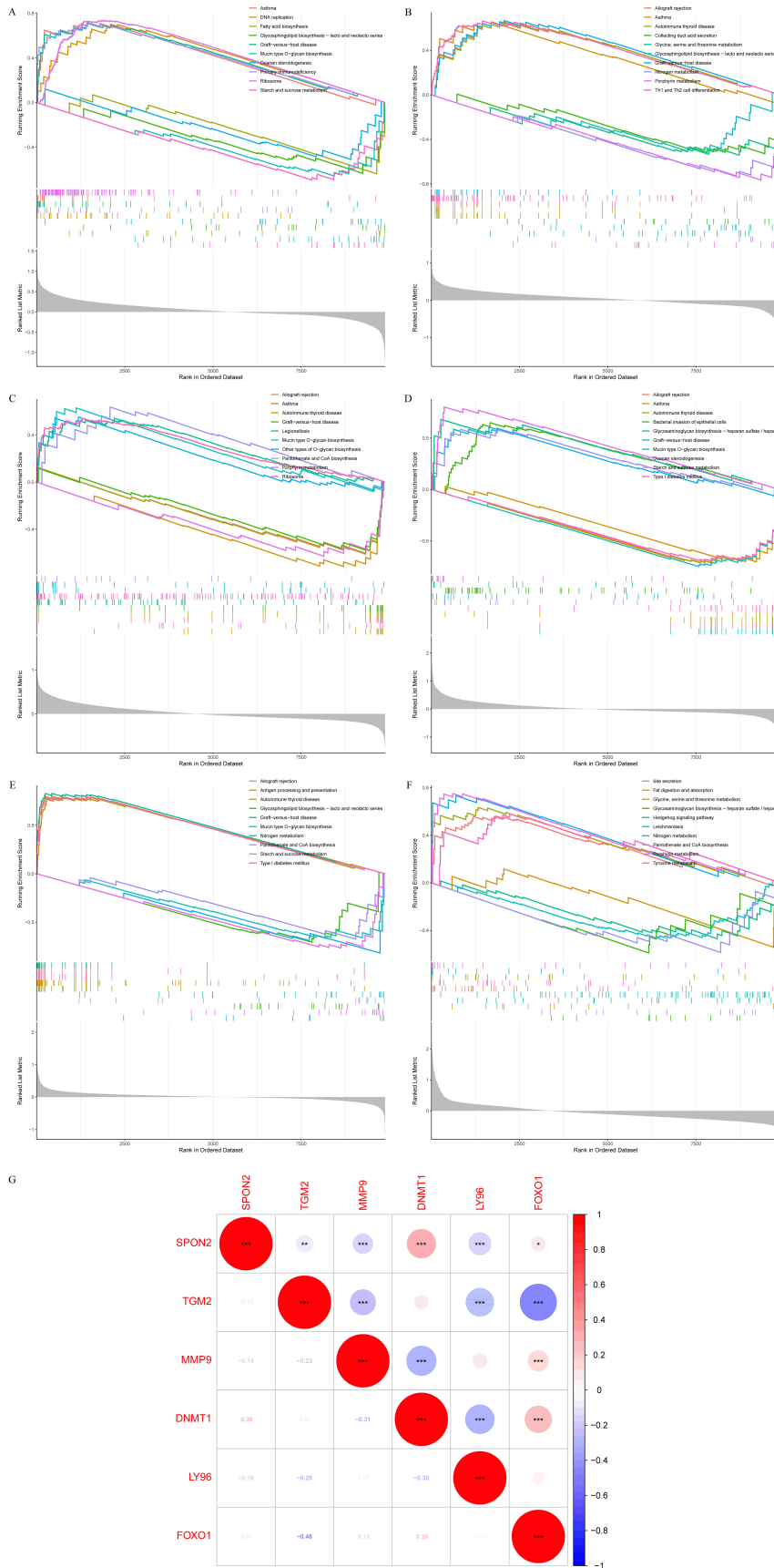


FIGURE 4. GSEA of hub genes. (A) *DNMT1*, (B) *FOXO1*, (C) *LY96*, (D) *MMP9*, (E) *SPON2*, (F) *TGM2* and (G) the correlation map of these six hub genes. * $p < 0.05$; ** $p < 0.01$; *** $p < 0.001$. GSEA, gene set enrichment analysis; *DNMT1*, DNA methyltransferase 1; *FOXO1*, forkhead box protein 1; *LY96*, lymphocyte antigen 96; *MMP9*, matrix metalloproteinase 9; *SPON2*, spondin 2; *TGM2*, transglutaminase 2.

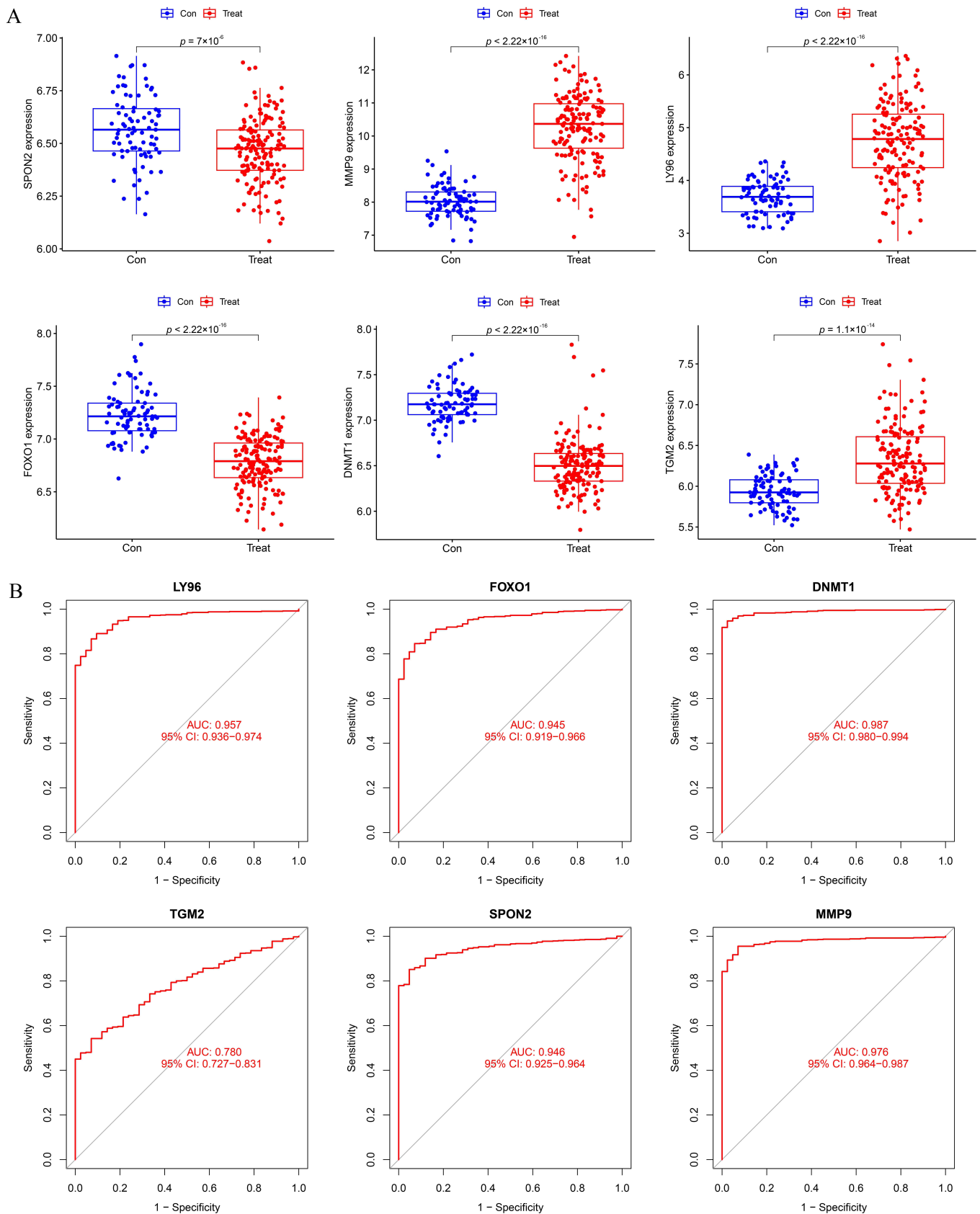


FIGURE 5. Hub gene expression in verification set. (A) Hub gene expression levels. **(B)** ROC curves of the six hub genes in the GSE134347 dataset. ROC, receiver operating characteristic. AUC, area under the curve; CI, confidence interval; *SPON2*, spondin 2; *MMP9*, matrix metalloproteinase 9; *TGM2*, transglutaminase 2; *DNMT1*, DNA methyltransferase 1; *FOXO1*, forkhead box protein 1; *LY96*, lymphocyte antigen 96.

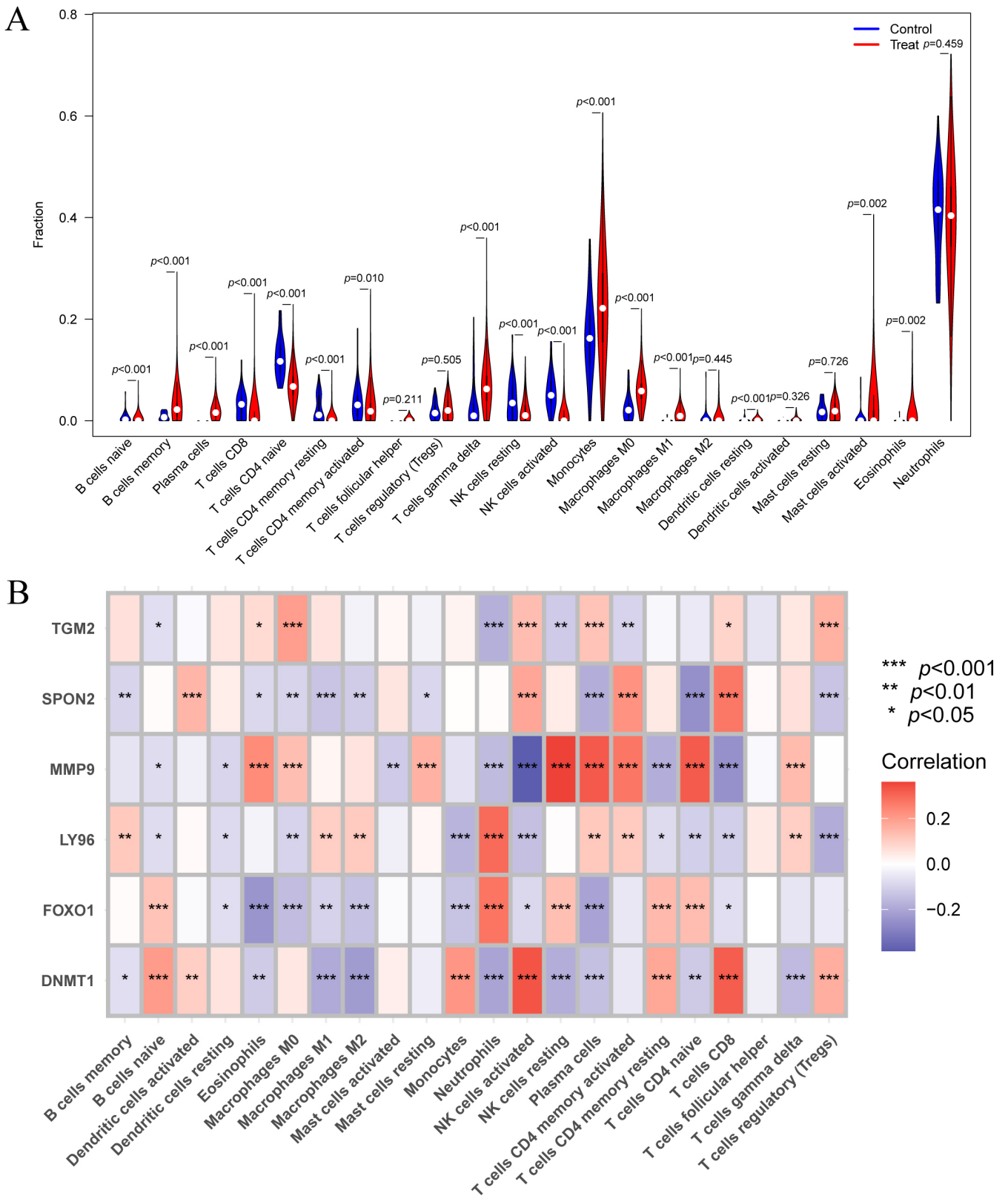


FIGURE 6. Immune cell infiltration analysis. (A) Differential infiltration of immune cells between the normal and disease groups. (B) Correlation heatmap between the six hub genes and the immune cells. * $p < 0.05$; ** $p < 0.01$; *** $p < 0.001$. NK, natural killer; CD, cluster of differentiation. *SPON2*, spondin 2; *MMP9*, matrix metalloproteinase 9; *TGM2*, transglutaminase 2; *DNMT1*, DNA methyltransferase 1; *FOXO1*, forkhead box protein 1; *LY96*, lymphocyte antigen 96.

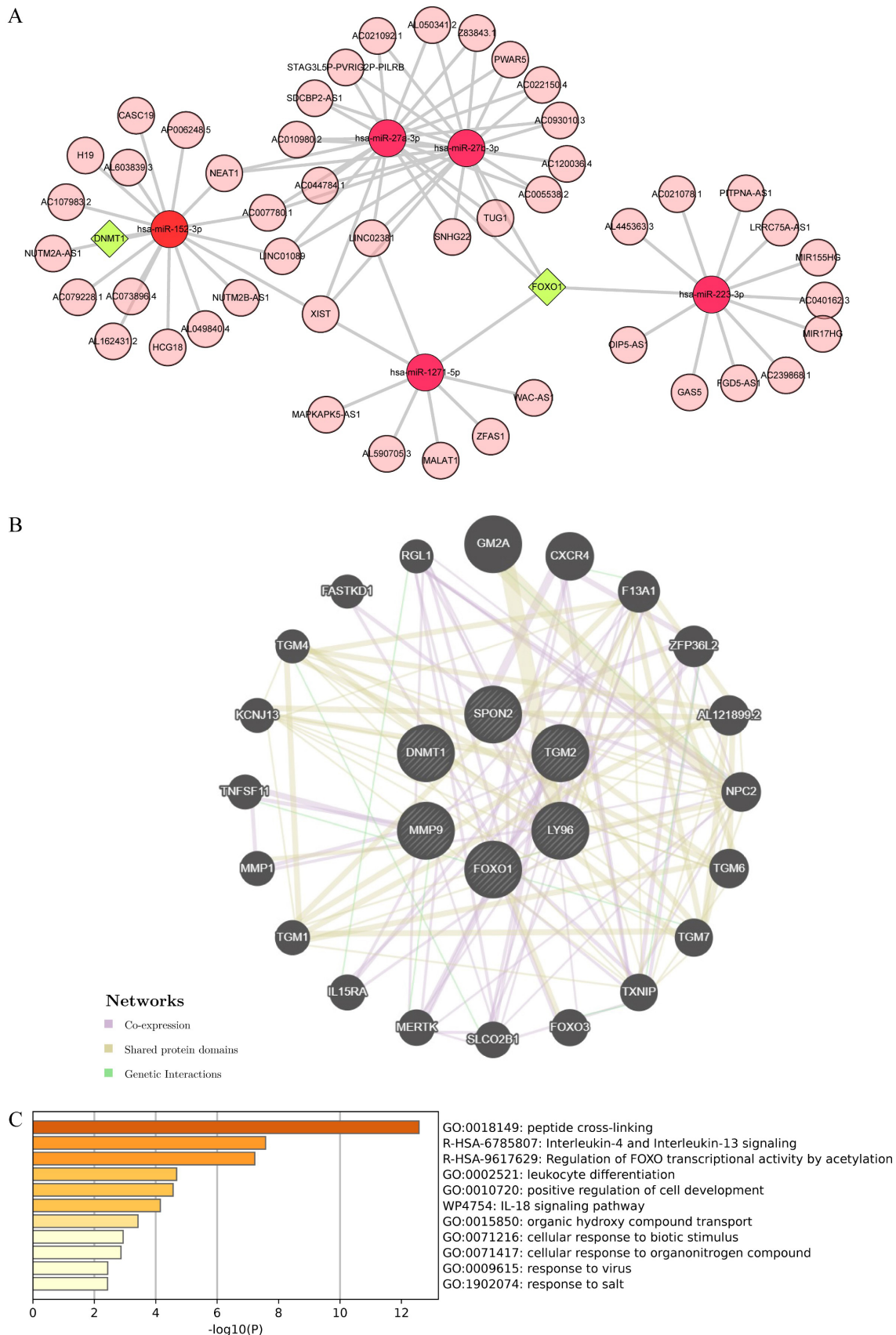


FIGURE 7. ceRNA regulatory network of the hub genes. (A) ceRNA network of the hub genes (pink circles represent lncRNAs, red circles represent miRNAs, and green diamonds represent the hub genes). (B) Hub gene co-expression network. (C) Enrichment analysis of gene functions in the co-expression network. ceRNA, competing endogenous RNA; lncRNA, long non-coding RNA; miRNA, micro-RNA; *SPON2*, spondin 2; *MMP9*, matrix metalloproteinase 9; *TGM2*, transglutaminase 2; *DNMT1*, DNA methyltransferase 1; *FOXO1*, forkhead box protein 1; *LY96*, lymphocyte antigen 96.

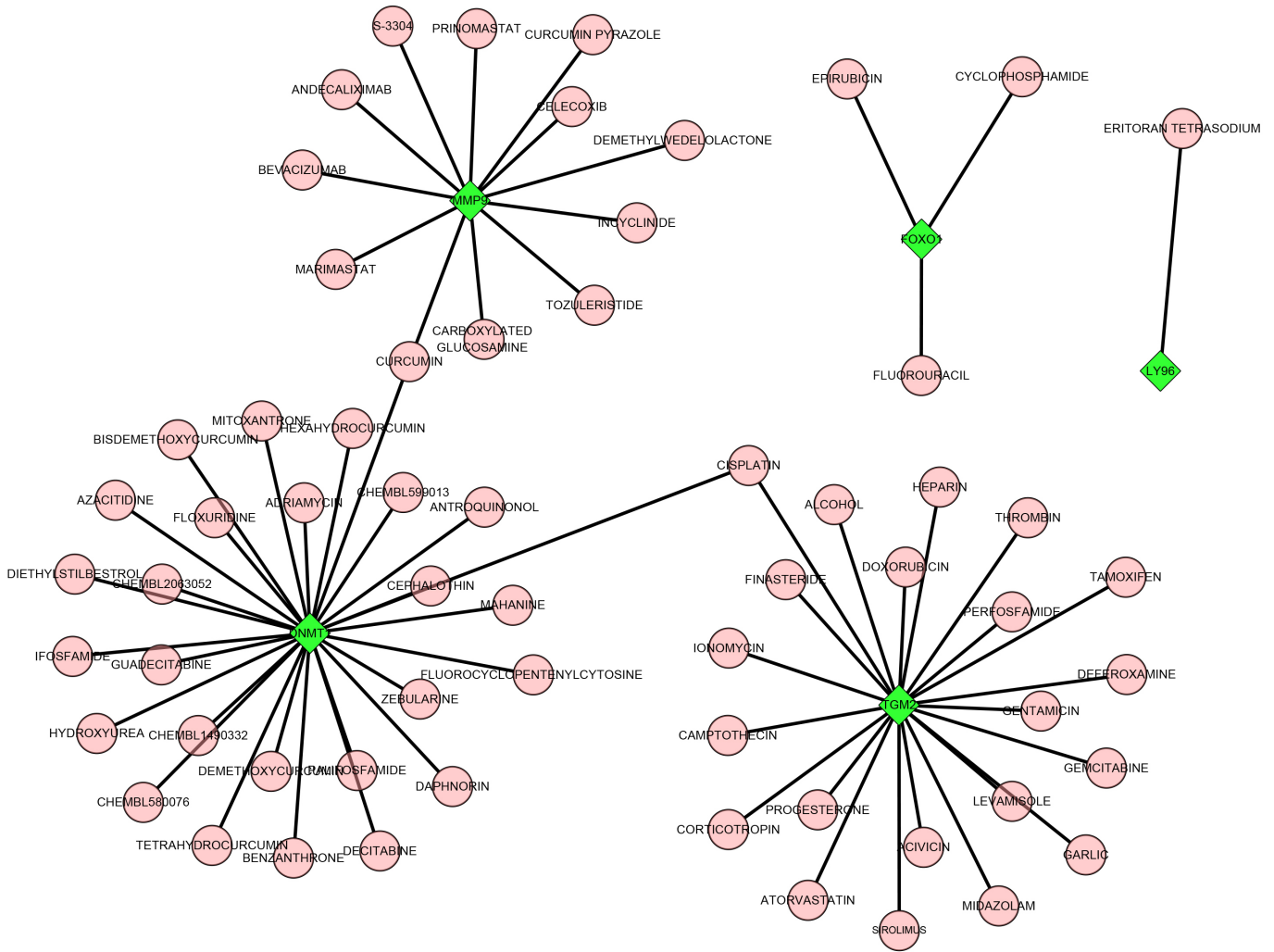


FIGURE 8. The predicted drug network. Green diamonds represent hub genes; pink circles represent interactive drugs. *MMP9*, matrix metalloproteinase 9; *TGM2*, transglutaminase 2; *DNMT1*, DNA methyltransferase 1; *FOXO1*, forkhead box protein 1; *LY96*, lymphocyte antigen 96.

4. Discussion

Sepsis, caused by an imbalance in the host’s immune response to infection, is a life-threatening condition characterized by organ dysfunction and a high mortality rate [14]. During chromatin remodeling, the final step of epigenetic regulation, a specific chromatin condensation state, is achieved, allowing the activity of chromatin remodeling agents at particular genomic sites [5, 6]. Epigenetic modifications play crucial roles in regulating sepsis immunity, particularly contributing to immunosuppression during the late stages of the disease [7, 8]. Thus, understanding the pathogenesis of sepsis is essential for developing new diagnostic and therapeutic strategies.

In this study, through a series of bioinformatic analyses on sepsis data from the Gene Expression Omnibus (GEO) and CRRGs identified from the GeneCards database, we used LASSO regression, SVM-recursive feature elimination, and random forest methods to screen six biomarker genes: *SPON2*, *TGM2*, *MMP9*, *DNMT1*, *LY96* and *FOXO1*. The infiltration of 16 types of immune cells differed significantly between the normal and disease groups. The six hub genes were significantly correlated with activated NK cells, CD8

T cells, and plasma cells. Additionally, *TGM2* and *MMP9* were significantly correlated with macrophages. Sepsis is closely related to immune dysfunction. Spondin 2 (*SPON2*), an extracellular matrix glycoprotein, plays an important role in the synthesis, degradation, and distribution of extracellular matrix components, which are important in disease occurrence and tumor progression. *SPON2* acts as a congenital host immunomodulator, recruiting macrophages and neutrophils during inflammation [15]. *SPON2* is up-regulated in many tumors and is associated with poor prognosis in patients with prostate, hepatocellular, and lung adenocarcinoma [16]. Experiments have shown that mice deficient in the *SPON2* gene could not resist septic shock caused by lipopolysaccharide, and their ability to clear bacterial infection was severely damaged [17]. *CXCR4*, which is highly correlated with *SPON2*, enhances the phagocytosis of mononuclear macrophages in sepsis [18]. In many animal models, *CXCR4* replicated naive CD4⁺ and CD8⁺ T cells and CD4⁺ central memory T cells selectively, thereby alleviating immune cell failure [19]. Human tissue transglutaminase (*TGM2*) is a multifunctional enzyme with transglutaminase crosslinking, G protein signaling, and kinase activities, playing important roles in many disease states and

mediating histone transglutaminization [20]. The chromatin nucleosome structure, which can inhibit *TGM2* activity, limits the space-accessible glutamine of the histone tail [21]. Defects in *TGM2* result in abnormalities in clearing apoptotic cells, leading to immune dysfunction and inflammation. Sepsis has been shown to cause immune dysfunction, preventing the body from mounting a normal immune response [22]. *TGM2* inhibits the c-Jun N-terminal kinase/Bcl-2 signaling pathway by interacting with aspartylglucosaminidase, thus alleviating lipopolysaccharide-induced apoptosis [22]. Lymphocyte antigen 96 (*LY96*) modulates host immunity by acting as an important cofactor in the recognition of microbial structural components of lipopolysaccharide by immune cells. High expression of *LY96* is related to a persistent pro-inflammatory immune response [23]. *FOXO1* belongs to the large family of forkhead transcription factors. *FOXO* transcription factors bind stably to target sites in the chromatin array of nucleosome and linker histone, which is indispensable for *FOXO* chromatin remodeling. Weigel and Jackle first reported *FOXO1* as a pivotal transcription factor due to its prominent role in regulating a wide range of biological processes, including cell proliferation, survival, DNA repair, cell cycle, apoptosis, metabolism, and immune regulation [24]. Increasing evidence suggests that miR-223 may limit inflammation to prevent collateral damage during infection, and *FOXO1* is a validated target for miR-223 [25]. Ji-Ding Fu *et al.* [26] found that atractylenolide III alleviated sepsis-mediated lung injury by inhibiting *FOXO1* and recombinant vanin 1.

Macrophages play essential roles in immune responses. Sepsis can induce macrophage apoptosis and inhibit their inflammatory responses. Normally, the expression of *MMPs* is low in the human body. However, during severe infection stress, *MMPs* are up-regulated by various inflammatory mediators released by activated inflammatory cells, such as monocytes, neutrophils and macrophages. These mediators are released into the blood, where they disrupt the basement membrane of endothelial cells, causing them to detach from the extracellular matrix, which damages the vascular wall, increases microvascular permeability, and raises the likelihood of sepsis [27]. Previous research showed that intracellular pathogens, viruses, and fungi induce the expression of host *MMPs*, suggesting that *MMPs* may be a potential therapeutic target in sepsis, which aligns with our results [28]. The diagnostic value of *MMP9* in sepsis has also been previously reported [29, 30]. DNA methylation is influenced by DNA methyltransferase activity, gene polymorphism, histone methylation status, RNA interference, and other factors. *DNMT1* can bind to active proteins and participate in transcription regulation and chromatin modification [31]. Fubing Ma *et al.* [32] found that *SMAD2* could directly bind to *DNMT1*, leading to miR-145 promoter hypermethylation, miR-145 downregulation, and *TGFBR2* upregulation. The *TGFBR2/SMAD2/DNMT1/miR-145* negative regulatory loop was shown to be responsible for lipopolysaccharide-induced sepsis [32].

This study had some limitations. Firstly, these results are yet to be validated *in vitro* experiments. Secondly, the exact mechanisms underlying the immune responses induced by *SPON2*, *DNMT1* and *LY96* need further elucidation. Therefore, these

findings should be verified through both *in vitro* experiments and clinical practice.

5. Conclusions

This study identified potential biomarkers for improving the diagnosis of sepsis and explored the role of immune cell infiltration in the progression of the disease. We established that six biomarkers (*SPON2*, *TGM2*, *MMP9*, *DNMT1*, *LY96* and *FOXO1*) might serve as potential targets for the diagnosis and treatment of sepsis. Additionally, we constructed a ceRNA network and identified potentially significant therapeutic drugs for improving patient outcomes based on these biomarkers.

AVAILABILITY OF DATA AND MATERIALS

All data included in this study are available upon request by contact with the corresponding author.

AUTHOR CONTRIBUTIONS

ZHZ—designed the project. ZHZ, YSM, NL, LFX, WX, YMZ, ZHC and BL—performed the experiments. ZHZ, YSM, YH, XCQ, LH, LL and JRD—discussed the results. YSM and LFX—wrote the manuscript. All authors reviewed the manuscript. All authors read and approved the final manuscript.

ETHICS APPROVAL AND CONSENT TO PARTICIPATE

Not applicable.

ACKNOWLEDGMENT

Thanks to all the peer reviewers for their opinions and suggestions.

FUNDING

The article supported by the Fundamental Research Funds for the Central Universities (226-2023-00123).

CONFLICT OF INTEREST

The authors declare no conflict of interest.

REFERENCES

- [1] Tang Y, Yang X, Shu H, Yu Y, Pan S, Xu J, *et al.* Bioinformatic analysis identifies potential biomarkers and therapeutic targets of septic-shock-associated acute kidney injury. *Hereditas*. 2021; 158: 13.
- [2] van der Poll T, van de Veerdonk FL, Scicluna BP, Netea MG. The immunopathology of sepsis and potential therapeutic targets. *Nature Reviews Immunology*. 2017; 17: 407–420.
- [3] Zhu T, Su Q, Wang C, Shen L, Chen H, Feng S, *et al.* SDF4 Is a prognostic factor for 28-days mortality in patients with sepsis via negatively regulating ER stress. *Frontiers in Immunology*. 2021; 12: 659193.

- [14] Cohen J, Vincent J, Adhikari NKJ, Machado FR, Angus DC, Calandra T, *et al.* Sepsis: a roadmap for future research. *The Lancet Infectious Diseases*. 2015; 15: 581–614.
- [15] Tammen SA, Friso S, Choi S. Epigenetics: the link between nature and nurture. *Molecular Aspects of Medicine*. 2013; 34: 753–764.
- [16] Falcão-Holanda RB, Brunialti MKC, Jasiulionis MG, Salomão R. Epigenetic regulation in sepsis, role in pathophysiology and therapeutic perspective. *Frontiers in Medicine*. 2021; 8: 685333.
- [17] Wu D, Shi Y, Zhang H, Miao C. Epigenetic mechanisms of immune remodeling in sepsis: targeting histone modification. *Cell Death & Disease*. 2023; 14: 112.
- [18] Cross D, Drury R, Hill J, Pollard AJ. Epigenetics in sepsis: understanding its role in endothelial dysfunction, immunosuppression, and potential therapeutics. *Frontiers in Immunology*. 2019; 10: 1363.
- [19] Yang X, Feng J, Liang W, Zhu Z, Chen Z, Hu J, *et al.* Roles of SIRT6 in kidney disease: a novel therapeutic target. *Cellular and Molecular Life Sciences*. 2022; 79: 53.
- [10] Lee SW, Park HJ, Jeon J, Park YH, Kim TC, Jeon SH, *et al.* Chromatin regulator SRG3 overexpression protects against LPS/D-GalN-induced sepsis by increasing IL10-producing macrophages and decreasing IFN γ -producing NK cells in the liver. *International Journal of Molecular Sciences*. 2021; 22: 3043.
- [11] Colaprico A, Silva TC, Olsen C, Garofano L, Cava C, Garolini D, *et al.* TCGAAbiolinks: an R/Bioconductor package for integrative analysis of TCGA data. *Nucleic Acids Research*. 2016; 44: e71.
- [12] Wu T, Hu E, Xu S, Chen M, Guo P, Dai Z, *et al.* clusterProfiler 4.0: a universal enrichment tool for interpreting omics data. *Innovation*. 2021; 2: 100141.
- [13] Chang YC, Su CY, Chen MH, Chen WS, Chen CL, Hsiao M. Secretory RAB GTPase 3C modulates IL6-STAT3 pathway to promote colon cancer metastasis and is associated with poor prognosis. *Molecular Cancer*. 2017; 16: 135.
- [14] Wang W, Liu C. Sepsis heterogeneity. *World Journal of Pediatrics*. 2023; 19: 919–927.
- [15] Huang C, Ou R, Chen X, Zhang Y, Li J, Liang Y, *et al.* Tumor cell-derived SPON2 promotes M2-polarized tumor-associated macrophage infiltration and cancer progression by activating PYK2 in CRC. *Journal of Experimental & Clinical Cancer Research*. 2021; 40: 304.
- [16] Lu H, Feng Y, Hu Y, Guo Y, Liu Y, Mao Q, *et al.* Spondin 2 promotes the proliferation, migration and invasion of gastric cancer cells. *Journal of Cellular and Molecular Medicine*. 2020; 24: 98–113.
- [17] He YW, Li H, Zhang J, Hsu CL, Lin E, Zhang N, *et al.* The extracellular matrix protein mindin is a pattern-recognition molecule for microbial pathogens. *Nature Immunology*. 2004; 5: 88–97.
- [18] Lai X, Ding H, Yu R, Bai H, Liu Y, Cao J. CXCL14 protects against polymicrobial sepsis by enhancing antibacterial functions of macrophages. *American Journal of Respiratory Cell and Molecular Biology*. 2022; 67: 589–601.
- [19] Ramonell KM, Zhang W, Hadley A, Chen CW, Fay KT, Lyons JD, *et al.* CXCR4 blockade decreases CD4⁺ T cell exhaustion and improves survival in a murine model of polymicrobial sepsis. *PLOS ONE*. 2017; 12: e0188882.
- [20] Lai TS, Greenberg CS. TGM2 and implications for human disease: role of alternative splicing. *Frontiers in Bioscience*. 2013; 18: 504–519.
- [21] Lukasak BJ, Mitchener MM, Kong L, Dul BE, Lazarus CD, Ramakrishnan A, *et al.* TGM2-mediated histone transglutamination is dictated by steric accessibility. *Proceedings of the National Academy of Sciences of the United States of America*. 2022; 119: e2208672119.
- [22] Zhang S, Fu B, Xiong Y, Zhao Q, Xu S, Lin X, *et al.* Tgm2 alleviates LPS-induced apoptosis by inhibiting JNK/BCL-2 signaling pathway through interacting with Aga in macrophages. *International Immunopharmacology*. 2021; 101: 108178.
- [23] Nie K, Li J, Peng L, Zhang M, Huang W. Pan-cancer analysis of the characteristics of LY96 in prognosis and immunotherapy across human cancer. *Frontiers in Molecular Biosciences*. 2022; 9: 837393.
- [24] Remadevi V, Muraleedharan P, Sreeja S. FOXO1: a pivotal pioneer factor in oral squamous cell carcinoma. *American Journal of Cancer Research*. 2021; 11: 4700–4710.
- [25] Haneklaus M, Gerlic M, O'Neill LA, Masters SL. miR-223: infection, inflammation and cancer. *Journal of Internal Medicine*. 2013; 274: 215–226.
- [26] Fu JD, Gao CH, Li SW, Tian Y, Li SC, Wei YE, *et al.* Atractylenolide III alleviates sepsis-mediated lung injury *via* inhibition of FoxO1 and VNN1 protein. *Acta Cirurgica Brasileira*. 2021; 36: e360802.
- [27] Yáñez-Mó M, Siljander PR, Andreu Z, Zavec AB, Borràs FE, Buzas EI, *et al.* Biological properties of extracellular vesicles and their physiological functions. *Journal of Extracellular Vesicles*. 2015; 4: 27066.
- [28] Fiotti N, Mearelli F, Di Girolamo FG, Castello LM, Nunnari A, Di Somma S, *et al.* Genetic variants of matrix metalloproteinase and sepsis: the need speed study. *Biomolecules*. 2022; 12: 279.
- [29] Lu X, Xue L, Sun W, Ye J, Zhu Z, Mei H. Identification of key pathogenic genes of sepsis based on the Gene Expression Omnibus database. *Molecular Medicine Reports*. 2018; 17: 3042–3054.
- [30] Xu C, Xu J, Lu L, Tian W, Ma J, Wu M. Identification of key genes and novel immune infiltration-associated biomarkers of sepsis. *Innate Immunity*. 2020; 26: 666–682.
- [31] Vanyushin BF. Enzymatic DNA methylation is an epigenetic control for genetic functions of the cell. *Biochemistry*. 2005; 70: 488–499.
- [32] Ma F, Li Z, Cao J, Kong X, Gong G. A TGFBR2/SMAD2/DNMT1/miR-145 negative regulatory loop is responsible for LPS-induced sepsis. *Biomedicine & Pharmacotherapy*. 2019; 112: 108626.

How to cite this article: Yansong Miao, Ning Liu, Lifeng Xing, Bing Li, Wei Xiao, Junru Dai, *et al.* Identifying six chromatin remodeling-related genes as diagnostic biomarkers in sepsis using bioinformatic analyses. *Signa Vitae*. 2025; 21(5): 1–13. doi: 10.22514/sv.2025.060.